I R A M P
4(2), December 2013, pp. 93-104

ISSN: 2229-3159

Spectroscopic Diagnostics of Non-Thermal Electrons with High-Number-Harmonic EC Radiation in Fusion-Reactor Plasmas

P. V. MINASHIN AND A. B. KUKUSHKIN

Tokamak Physics Institute, NRC "Kurchatov Institute", Moscow, Russia

ABSTRACT: A method of spectroscopic diagnostics of the average transverse-to-magnetic-field momentum of the non-thermal component of the electron velocity distribution (EVD), based on the high-number-harmonic electron cyclotron (EC) radiation, is suggested for nuclear fusion-reactor plasmas under condition of a strong auxiliary heating (e.g. in tokamak DEMO, a next step after tokamak ITER). The method is based on solving an inverse problem for reconstruction of the EVD in parallel and perpendicular to magnetic field components of electron momentum at high and moderate energies responsible for the emission of the high-number-harmonic EC radiation.

1. INTRODUCTION

Spectroscopic diagnostics of electron temperature from the low EC harmonics of thermal EC radiation is widely used in the facilities for magnetic confinement of high-temperature plasmas (tokamaks, stellarators). In tokamaks, the diagnostics is based on the (approximate) one-to-one correspondence between three quantities: toroidal major radial coordinate, toroidal magnetic field, and EC frequency of registered radiation [1], [2]. For low-number harmonics of fundamental cyclotron frequency (usually, the 1st and 2nd ones) the emitted EC radiation is strongly trapped in a rather thin layer of plasma on the line-of-sight (usually, perpendicularly to the toroidal magnetic field) of the detector. For thermodynamic equilibrium (Maxwellian velocity distribution for electrons) one has similar equilibrium (Planck distribution) for radiation intensity which – for the smallness of wave quantum energy as compared to temperature (that is definitely valid for EC radiation) – reduces to Rayleigh-Jeans direct proportionality between intensity and temperature. Thus, the frequency profile of the registered thermal radiation at a certain low-number harmonic appears to give the line-of-sight profile of electron temperature. The deviations of electron velocity distribution from a Maxwellian distort this correspondence and may be a source of sometimes observed difference of temperature values inferred from the local spectrum of the laser radiation Thomson scattering and the EC radiation intensity at the respective point of plasma. However, the non-Maxwellian effects are relatively small for the frequency domain where thermal EC radiation dominates.

The strong effects of a non-Maxwellian EVD may be observed at the relativistically down-shifted frequencies (including those lower than the 1st and 2nd harmonic for the low-magnetic-field side of tokamak plasma) where the EC radiation is dominated by the fast, non-thermal electrons at the periphery where the EC radiation emitted at these frequencies may escape from plasma. An example of treating these effects for the reconstruction of an essentially non-Maxwellian EVD may be found in [3], [4] for interpretation of the data from tokamak T-10. However, the use of this effect for diagnostics of the edge plasma in fusion reactors is possible only in regimes with low plasma density at the plasma edge.

The studies of non-Maxwellian effects at EC harmonics $n > 2$ have a long history, see e.g. [5]. The complexity of this case stems from several issues: the transient regime of radiation transfer, namely, from optical thickness (strong trapping of ECR) at EC harmonics $n = 1$ and $n = 2$ to optical transparency at high-number harmonics;

a decrease of the spectral gap between, and overlapping of the neighboring harmonics of the thermal EC radiation. In tokamak-reactors one has a simplification in the sense that for $n > 3$ the EC radiation has the following features: (a) the spectrum of outgoing EC radiation is a smooth function, due to a strong overlapping of harmonics in a high-temperature fusion plasma and (b) the radiative transfer at the frequencies which are most important for EC radiation losses, takes place in the regime of a low optical thickness and strong reflections from the first wall [6], [7], [8], [9]. The latter, however, makes the radiative transport essentially nonlocal, and the identification of non-Maxwellian effects is feasible mainly for central plasma, with the highest temperature, because only this radiation has a peculiar spectral range (namely, high-number harmonics) in the spectrum of outgoing radiation.

In contrast to the present day tokamaks, the EC wave emission by the plasma can significantly contribute to the local electron power balance in central part of plasma column for high temperatures expected in DEMO and steady-state regimes of ITER operation (see, e.g., [10], [11]). When central temperature increases to $T_e(0) \sim 30$ keV the local EC power loss becomes a substantial part of heating from fusion alpha-particles and is close to the total auxiliary heating. Also, the fast increase of the EC losses with increasing temperature may have a positive impact on stabilization of fusion burning [12], keeping fusion power and divertor loads at moderate level for all imaginary temperature excursions, that is important for long pulse operation scenarios [13]. These conclusions have been made in the frame of modeling with the neglect of deviations of the EVD from a Maxwellian. The impact of possible deviations of the EVD from a Maxwellian on the EC power losses has been analyzed in [14], [15], [16]. First self-consistent calculations of the plasma-produced EC radiation and superthermal electron kinetics was carried out in [17]. The problem of self-consistent modeling of electron kinetics, EC wave propagation and EC power losses in tokamaks is discussed in [18] (see also references therein). This assumes using the Fokker-Planck codes for numerical modeling of electron kinetics (e.g. the CQL3D code [19]) with allowance for both the injected EC wave at low number harmonics and the plasma-produced EC radiation which in tokamak-reactors is dominant at moderate- and high-number EC harmonics. An example of using the CQL3D for interpretation of diagnostic data (non-Maxwellian effects in the Thomson scattering in tokamak TCV under ECRH and ECCD conditions) may be found in [20]. In general, one has to combine various diagnostic data to reconstruct the deviations of the EVD from a Maxwellian.

In the present paper, we suggest a new method of spectroscopic diagnostics of the average transverse-to-magnetic-field momentum of the non-thermal component of the EVD, based on the high-number harmonic EC radiation from nuclear fusion-reactor plasmas under condition of a strong auxiliary heating (e.g. in tokamak DEMO, a next step after tokamak ITER). The method is based on solving an inverse problem for reconstruction of the EVD in parallel and perpendicular to magnetic field components of electron momentum at high and moderate energies responsible for the emission of the high-number-harmonic EC radiation.

2. DIAGNOSTICS OF ELECTRON TEMPERATURE FROM EC RADIATION SPECTRUM FOR MAXWELLIAN PLASMAS

We start our consideration with an analysis of the possibility to diagnose the electron temperature of the central hot plasma in a fusion reactor from the EC radiation spectrum for purely Maxwellian plasmas. In this case it is possible to observe the impact of central temperature on the EC spectrum in a certain range of frequencies. One can expect the dependence of spectrum's slope with increasing frequency on the absolute value of the central temperature. We illustrate this effect on the example of a variation of the electron temperature profile around that obtained in [21] for self-consistent modeling of plasma parameters in a DEMO-type tokamak, with the help of the CRONOS suite of codes [22] for plasma equilibrium and transport modeling. The results of such an analysis are shown in figures 1-4.

To calculate the spectrum of the outgoing EC radiation we use the CYNEQ code [7], [23], [24] while the EXACTEC code [8] was used in the modeling [21]. Note that comparison of the codes for calculation of the power losses profiles was carried out in [25] and [26] for various representation of the effective magnetic field which is relevant to the existing practice of the 1D transport modeling of tokamak plasma (e.g., ASTRA [27] and CRONOS [22]). This field, $B(\rho)$, is obtained from the 2D magnetic field, $B(\rho, \theta)$, as a function of the normalized toroidal flux through the magnetic surface, ρ, and poloidal angle, θ, by averaging over magnetic flux surfaces. In [25] the benchmarking of the codes was done for $B(\rho)$ = const and given profiles of density and temperature,

whereas in [26] a comparison is made of the results obtained with account of the effects of 2D magnetic field and plasma equilibrium calculated self-consistently with plasma transport, including the EC power losses.

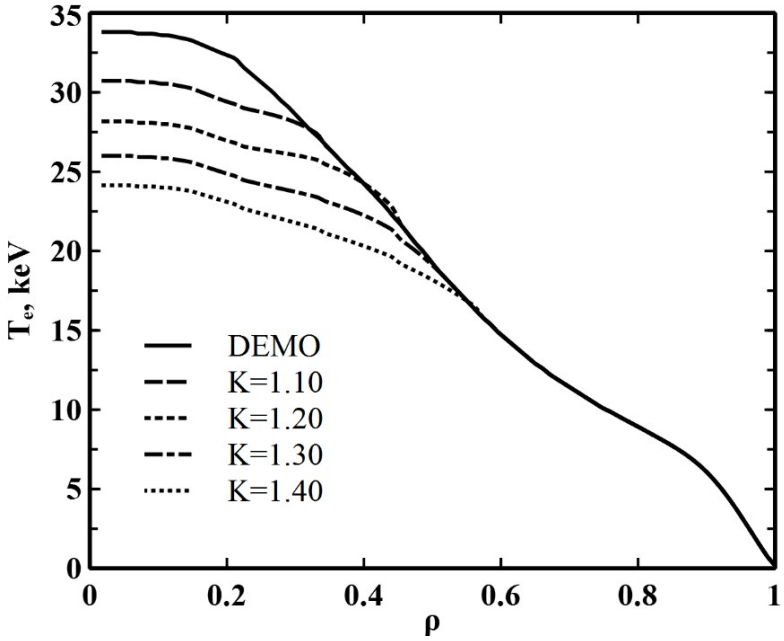

Figure 1: Electron temperature profile, T_e (ρ), for DEMO scenario 2 with EC heating and EC current drive [21] (solid line) predicted by the CRONOS code, and a set of hypothetical temperature profiles obtained from the above profile by a proportional decrease in the range ρ ≤ 0.5, T_e (ρ ≤ 0.5)/K, using a spline interpolation with the original profile for ρ > 0.5. Parameter ρ is a square root of the normalized toroidal magnetic flux. Global characteristics of DEMO operation scenarios [21]: major radius R_0 = 7.5 m, minor radius a = 2.5 m, elongation k_{elong} = 1.9, triangularity δ = 0.47, vacuum toroidal magnetic field on the toroidal axis of vacuum vessel B_0 = 6 T, plasma current I_p = 19 MA, electron density $n_e(0) = 1.3\ 10^{20}$ m^{-3}, $< n_e > = 1.0\ 10^{20}$ m^{-3}

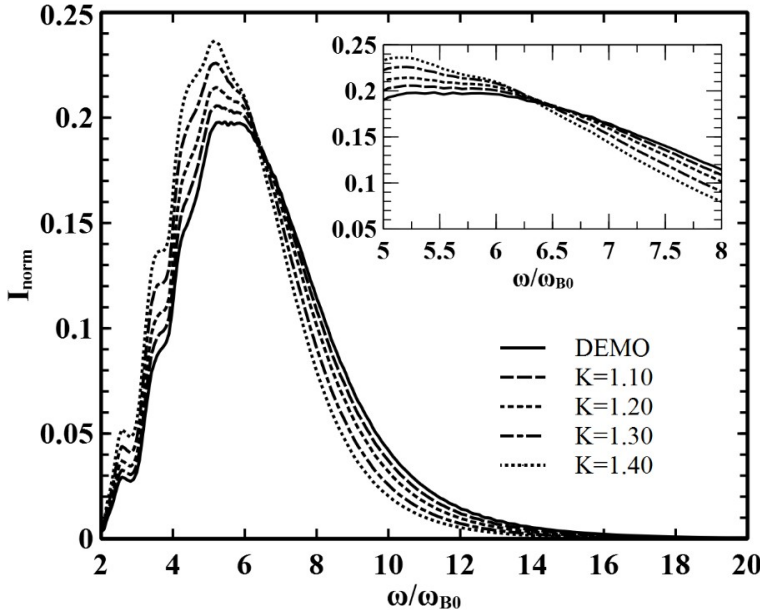

Figure 2: Normalized intensity of the outgoing EC radiation, I_{norm}, as a function of normalized frequency, ω/ω$_{B0}$ (ω$_{B0}$ is the fundamental EC frequency for magnetic field B_0), calculated by the CYNEQ code [7], [23], [24] for DEMO scenario 2 [21], R_w = 0.7 (solid line) and for the same parameters and modified T_e profiles (see Fig. 1). Inset shows in detail the range of frequencies important for the proposed spectroscopic diagnostics.

In the CYNEQ model [7], which modifies and improves the nonloñal EC radiation transport model [28], the intensity of the outgoing radiation is described by the following formula (the mixing of the modes, caused by wave reflection, is neglected):

$$I_{\rm esc}(\omega,\varsigma)=\frac{\left\langle\int\frac{d\Omega_n}{4\pi}\,q_\varsigma\left(\mathbf{r},\Phi\right)\right\rangle_{V_{\rm esc}}}{\int\frac{d\Omega_n}{4\pi}\int\frac{\mathbf{n}\cdot d\mathbf{S}_w}{V_{esc}}\left(1-R_w(\omega,\mathbf{n})\right)+\left\langle\int\frac{d\Omega_n}{4\pi}\,\kappa_\varsigma\left(\mathbf{r},\Phi\right)\right\rangle_{V_{\rm esc}}}, \tag{1}$$

$$I_{\rm esc}(\omega)=\sum_{\varsigma=X,O} I(\omega,\varsigma), \tag{2}$$

where $\Phi = (\omega, \mathbf{n}, \varsigma)$, ω and $\mathbf{n} = \mathbf{k}/k$ - wave frequency and direction of propagation, $\mathbf{k}$ - wave vector, index $\varsigma = X, O$ denotes respectively the extraordinary (X) and ordinary (O) wave types, $\kappa(\mathbf{r}, \phi)$ is the EC radiation absorption coefficient, $q(\mathbf{r}, \phi)$ is the power density of the EC radiation source, $V_{\rm esc}$ is a part of the plasma volume where the EC radiation can propagate almost without absorption, with taking into account the wave cut-off, $< >_{V_{\rm esc}}$ is an averaging over volume $V_{\rm esc}$, S_w - area of vacuum chamber inner surface (the surface integral in the denominator of the fractionis taken over the semi-sphere where $(\mathbf{n} \cdot dS_w) > 0$), R_w is reflection coefficient of the EC radiation from the wall.

It is seen from Figure 2 that there is a possibility to distinguish between various central temperatures in the range of frequency $5 \le \omega/\omega_{B0} \le 8$: here the slope of the spectrum shows a regular monotonic behavior. One can compare the respective values and restore the central temperature despite the slope (i.e. derivative) has substantial local fluctuations. However, the averaged values of the slope exhibit regular behavior (Figs. 3 and 4).

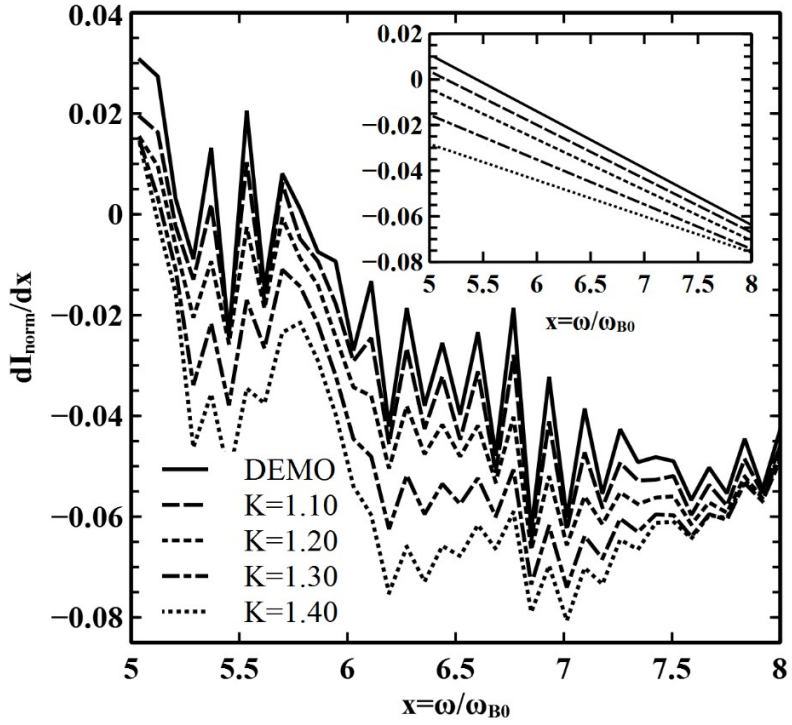

Figure 3: Derivative of the normalized intensity of the outgoing EC radiation from Fig. 2 with respect to its argument $x = \omega/\omega_{B0}$. The notations are the same as in Fig. 2. Also the linear least-square fitting of the curves is shown in the inset

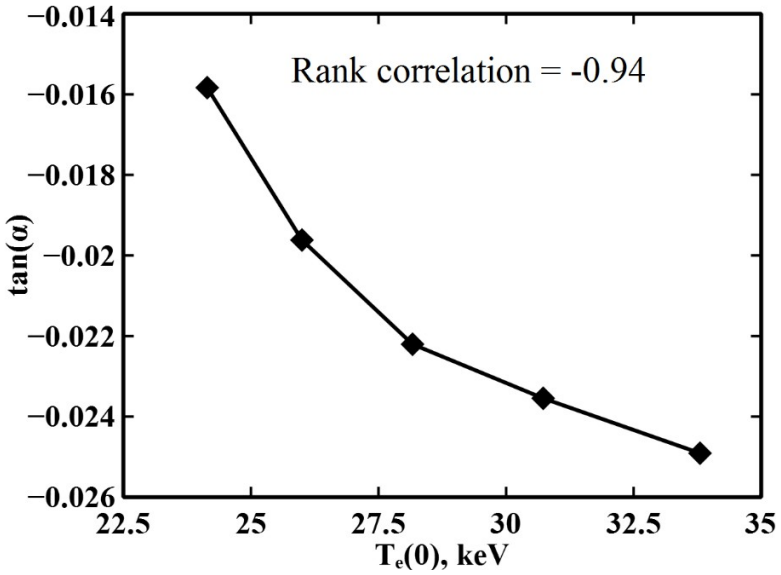

Figure 4: Correlation between central temperature, $T_e(0)$, and tan (α), the slope of the linear approximation of the derivative of the normalized intensity of the outgoing EC radiation in Fig. 3 in the range $5 \le \omega/\omega_{B0} \le 8$. The Pearson's linear correlation coefficient is equal to – 0.94

3. DIAGNOSTICS OF ELECTRON VELOCITY DISTRIBUTION PARAMETERS FROM EC RADIATION SPECTRUM IN FUSION-REACTOR NON-MAXWELLIAN PLASMAS

The optimistic conclusions of the previous section are based on the use of the known functional form of the EVD. In the case of arbitrary EVD the capability to reconstruct the main parameters of the EVD are restricted to those parameters, which are most sensitive to EC radiation, first of all, to average transverse-to-magnetic-field momentum of non-thermal electrons.

Numerical modeling of the EC radiation in the presence of an anisotropic distribution of superthermal electrons is carried out here with the modified CYNEQ code [7], [23], [24]. We assume the electron distribution function to be a sum of a Maxwellian distribution function for the bulk plasma and a *bi*-Maxwellian anisotropic distribution of superthermal electrons:

$$f(\rho, \mathbf{p}) = (1 - \delta_{\mathrm{Hot}}(\rho)) \cdot f_{\mathrm{Max}\,w}(\rho, \varepsilon) + \delta_{\mathrm{Hot}}(\rho) \cdot f_{\mathrm{Hot}}(\rho, p_{\|}, p_{\perp}), \tag{3}$$

$$f_{\mathrm{Hot}}(\rho, p_{\|}, p_{\perp}) = \mathrm{Const} \cdot \exp\left[- m_e c^2 \left(\frac{\sqrt{1+p^2} - 1}{p^2} \right) \left(\frac{p_{\|}^2}{T_{\|}(\rho)} + \frac{p_{\perp}^2}{T_{\perp}(\rho)} \right) \right], \tag{4}$$

$$\int f(\rho, \mathbf{p})\, d\mathbf{p} = n_e(\rho), \tag{5}$$

where **p** and ε is the momentum and the energy of an electron; signs ||, ⊥ denote parallel and perpendicular to the magnetic field components of a vector, respectively; $\delta_{\mathrm{Hot}}(\rho)$ and $T_{\|,\perp}(\rho)$ profiles are given by the formulas:

$$F(\rho) = (F)_{\max} EXP\left[- (\rho - \rho_0)^2 / (\Delta\rho)^2 \right], \; F = \left\{ T_{\perp,\|}, \delta_{\mathrm{Hot}} \right\}, \tag{6}$$

$$\begin{gathered} \rho_0 = 0, \qquad \Delta\rho = 0.3, \\ (\delta_{Hot})_{\max} = 0.1, \\ (T_{\|})_{\max} = 90\, keV, \quad (T_{\perp})_{\max} = 60\, keV \end{gathered} \tag{7}$$

The respective intensity of outgoing EC radiation exhibits the presence of a tail of the spectrum at high-number harmonics (Fig. 5).

The proposed spectroscopic diagnostics is based on the solution of an inverse problem for reconstruction of the

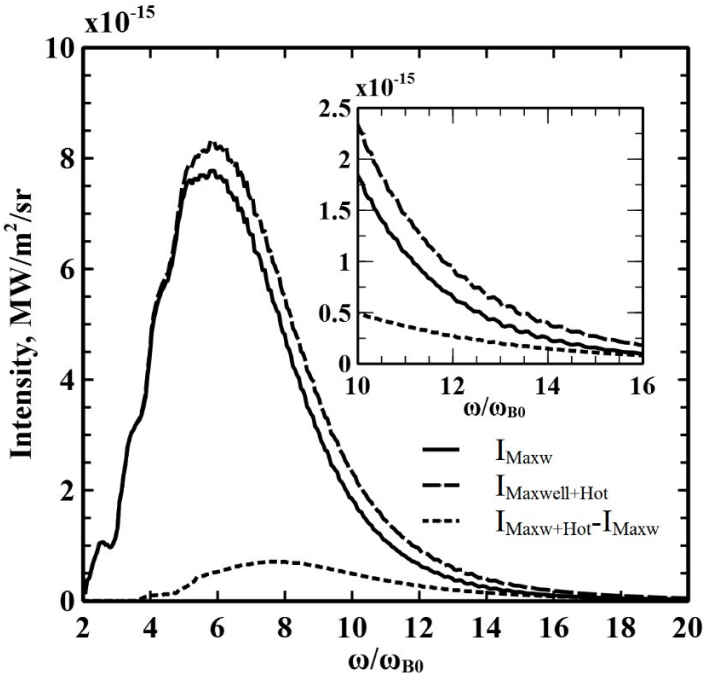

Figure 5: Intensity of the outgoing EC radiation, as a function of normalized frequency, ω/ω_{B0}, calculated by the CYNEQ code [7], [23], [24] for DEMO scenario 2 in Ref. [21] for the Maxwellian electron distribution function (solid line) and distribution function of eqs. (3)-(7) with the same parameters of the bulk Maxwellian and a fraction of superthermal electrons (dashed line). In addition, the difference between two spectra is shown (dotted line). Inset shows in more detail the range of frequencies, which are of interest to the proposed spectroscopic diagnostics

EVD in parallel and perpendicular to magnetic field components of electron momentum at high and moderate energies responsible for the emission of the high-number-harmonic EC radiation (similarly to the inverse problem solved in [3]). In such a formulation we assume that

- parameters of the EVD of the bulk Maxwellian plasma are known from other diagnostics, presumably, Thomson scattering, and
- we can determine parameters of the EVD only at high enough energy of electrons and actually only in the central plasma.

In the frame of the CYNEQ model the inverse problem is formulated as follows. For the high harmonics the intensity of the outgoing EC radiation, described by eqs. (1)-(7), may be simplified, due to a small absorption at these frequencies, and takes the form of a linear dependence of the measured intensity on the EVD of superthermal electrons:

$$I_{\mathrm{esc}}(\omega) = I_{\mathrm{esc}}^{\mathrm{Max}\,w}(\omega) + I_{\mathrm{esc}}^{\mathrm{Hot}}(\omega), \tag{8}$$

$$I_{\mathrm{esc}}^{\mathrm{Hot}}(\omega) = \sum_{\varsigma = X,\,\mathrm{O}} \frac{\int \frac{d\Omega_n}{4\pi}\, dV\, d\mathbf{p}\; q_{\varsigma}^{\mathrm{Hot}}\left(\mathbf{r}, \Phi\right)}{\int \frac{d\Omega_n}{4\pi} \int \mathbf{n} \cdot d\mathbf{S}_w \left(1 - R_w(\omega, \mathbf{n})\right)}, \tag{9}$$

$$\left\langle \frac{d\Omega_n}{4\pi} q_\varsigma^{Hot}(\mathbf{r},\Phi) \right\rangle_{V_{esc}} = \int \frac{dV}{V} d\mathbf{p} \left\langle \eta(\mathbf{r},\mathbf{p},\mathbf{n},\omega,\zeta) \right\rangle_{\Omega_n} \cdot \delta_{\mathrm{Hot}}(\rho) \cdot f_{\mathrm{Hot}}(\rho, p_{\|}, p_{\perp}), \tag{10}$$

where $I_{esc}(\omega)$ is the intensity of the outgoing EC radiation, $I_{esc}^{\mathrm{Max}\,w}(\omega)$ is the intensity for the Maxwellian EVD, $\eta(\mathbf{r}, \mathbf{p}, \mathbf{n}, \omega, \zeta)$ is the emissivity for a single electron, calculated using the Schott-Trubnikov formula (cf. [29], [1]). Note that for high harmonics of the EC fundamental frequency, V_{esc} in eq. (1) is equal to the total plasma volume, V. The direct problem — the calculation of the EC radiation spectra for a given EVD — is the calculation of eqs. (8)-(10) for known parameters of the bulk plasma and the superthermal electrons. The inverse problem assumes determination of the superthermal electron distribution function $\delta_{\mathrm{Hot}}(\rho)\, f_{\mathrm{Hot}}(\rho, \mathbf{p})$, for which the calculated spectrum $I_{esc}^{\mathrm{Hot}}(\omega)$ is a difference of the observed intensity $I_{esc}(\omega)$ and the calculated intensity $I_{esc}^{\mathrm{Max}\,w}(\omega)$ for the bulk plasma. Equations (8)-(10) can be rewritten in the following operator form:

$$Mf(\mathbf{r},\mathbf{p}) = I(\omega), \tag{11}$$

$$I(\omega) = I_{esc}(\omega) - I_{esc}^{\mathrm{Max}\,w}(\omega), \tag{12}$$

$$M = \left(\sum_{\varsigma = X,\,O} \frac{\int dV\, d\mathbf{p} \left\langle \eta(\mathbf{r},\mathbf{p},\mathbf{n},\omega,\zeta) \right\rangle_{\Omega_n}}{\int \frac{d\Omega_n}{4\pi} \int \mathbf{n} \cdot d\mathbf{S}_w \left(1 - R_w(\omega,\mathbf{n})\right)} \right), \tag{13}$$

where linear operator M is acting between the space $R_f = \{\rho, p_{\|}, p_{\perp}\}$, in which the EVD function is set ($f \in R_f$), and the space $Z = \{\omega\}$, in which the observed intensity is set ($I_{esc}(\omega) \in Z$). Because of the impossibility to invert the M operator (there is no unique solution) we solve this inverse problem using the optimization methods. We define the objective function that measures how good the calculated spectrum fits the observed data:

$$\phi(f) = \| Mf - I \|_Z^2, \tag{14}$$

which represents the L-2 norm, in Z-space, of the misfit between the predicted data and the observed data. The optimization problem with object function and nonnegative constrain is formulated as follows (nonnegative least squares):

$$\min_f \| Mf - I \|_Z^2, \quad f \geq 0 \tag{15}$$

The discretization of eqs. (11)-(14) on the grids in the $R_f = \{\rho, p_{\|}, p_{\perp}\}$ space and the $Z = \{\omega\}$ space, leads to the following formulas:

$$M_i f = \sum_k A_{ik} f_k, \tag{16}$$

$$\tilde{A}(\mathbf{r},\mathbf{p},\omega) = \frac{\sum_{\varsigma = X,\,O} \left\langle \eta(\mathbf{r},\mathbf{p},\mathbf{n},\omega,\zeta) \right\rangle_{\Omega_n}}{\frac{1}{4}(1 - R_w)\frac{S_w}{V}}, \tag{17}$$

$$A_{ik} = \tilde{A}(\omega_i, \Gamma_k)\frac{\Delta\Gamma_k}{V}, \tag{18}$$

where M_i is the discrete analog of the M operator , "k" numbers the phase-space cells in the $R_f = \{\rho, p_{\|}, p_{\perp}\}$ space, $\Delta\Gamma_k$ is the volume of the k-th cell, "i" is number of the point in the $Z = \{\omega\}$ space.

The inverse problem is an ill-posed one (the condition number of *A*-matrix is large, replacing *A* by a well-conditioned matrix derived from A does not lead to a useful solution due to the unknown errors in the observed spectra). The standard way to treat such ill-posed problems is to use the numerical regularization theory.

Here we show that if we incorporate additional information about the physics of EC radiation at high harmonics in the problem we can restore some parameters of the superthermal electrons. We shall consider the simplest case of 0D magnetic field in the 1D radiation transport model (namely, the magnetic-surface-average magnetic field is taken $B(\rho) = B_0$) and concentric circle magnetic surfaces, so that in eqs. (15)-(18) the function $\langle \eta(\rho, \mathbf{p}, \mathbf{n}, \omega, \zeta) \rangle_{\Omega_n}$ does not depend on the magnetic surface coordinate ρ. For this case the problem (8)-(10) can be solved in two steps:

- restoring the $q = q_\varsigma^{\mathrm{Hot}}(\rho, \omega)$ function from the observed spectra $I(\omega)$ via solving the inverse problem

$$\min_q \left\| M_\rho\, q - I \right\|_Z^2, \quad q \geq 0, \tag{19}$$

$$M_\rho\, q = \frac{2\int q(\rho, \omega)\rho d\rho}{\frac{1}{4}(1 - R_w)\frac{S_w}{V}} \tag{20}$$

- restoring the EVD function of superthemal electrons from $q = q_\varsigma^{\mathrm{Hot}}(\rho, \omega)$ via solving the inverse problem:

$$\min_f \left\| M_{\mathbf{p}}\, f - q \right\|_Z^2, \quad f \geq 0, \tag{21}$$

$$M_{\mathbf{p}}\, f = \sum_{\varsigma = X, \mathrm{O}} \int d\mathbf{p} \langle \eta(\mathbf{r}, \mathbf{p}, \mathbf{n}, \omega, \zeta) \rangle_{\Omega_n} f \tag{22}$$

As one can see, here the initial inverse problem (15)-(18) is divided in two inverse problems (19)-(20) and (21)-(22), related via the operator $M = M_\rho M_{\mathbf{p}}$.

Assuming that the most significant contribution to the spectra comes from superthermal electrons located near the ρ = 0 surface, we can start directly with the 2-nd task.

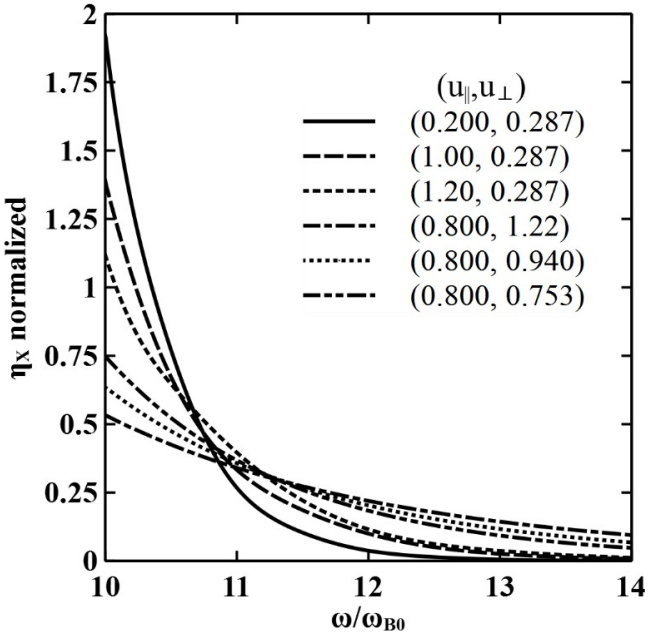

(a)

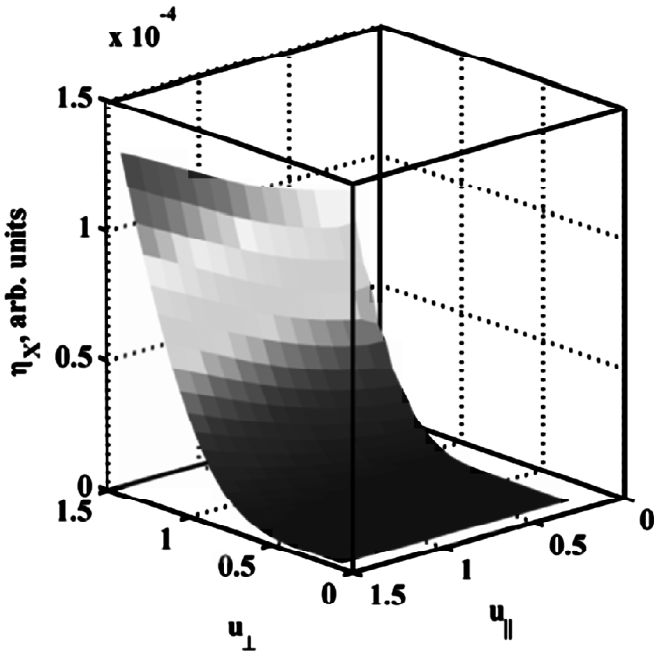

(b)

Figure 6:(a) Emissivity for the X-mode of EC radiation from a single electron, in the units of $e^2\omega^2/(2\pi\,\omega_{B0}\,c)$ (*c*-speed of light), averaged over the photon angles, as a function of normalized frequency for different values of ($p_\parallel$, $p_\perp$). The function is normalized to its integral in the ω-space. (b) The same as in figure "*a*" but in the 3D view, as a function of the u = p/*mc* vector components, for a fixed normalized frequency ω/ω_{B0} = 12

We illustrate the capability of the above algorithm on the example of the $I_{\rm esc}^{{\rm Max}\,w}(\omega)$ for bulk plasma taken again from [21], and a superthermal plasma with parameters (4), (6)-(7). The results of such an analysis are shown in Figures 6-9 where for simplicity we consider the X-mode of EC radiation which dominates in the observed signal.

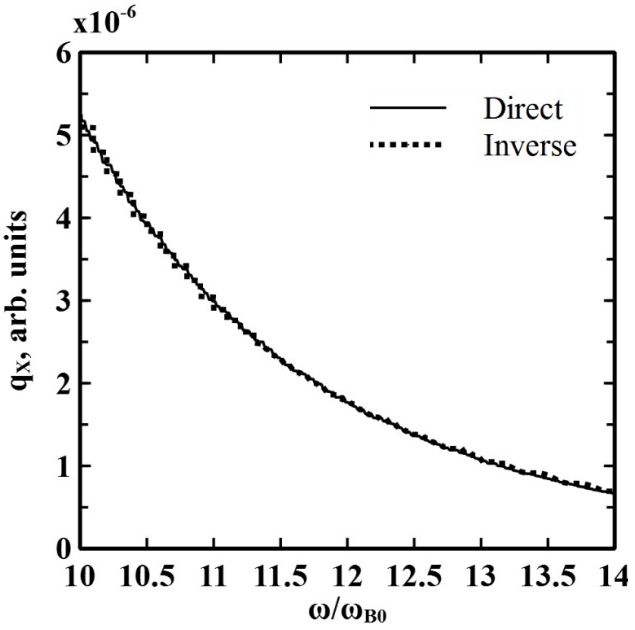

Figure 7: The power density of the spontaneous EC radiation source for the *X*-mode (in the units of $e^2\omega^2/(2\pi\,\omega_{B0}\,c)$): direct calculation by the CYNEQ code for superthermal EVD (4), (6), (7), which is used as a synthetic input (i.e. "phantom" experimental) data for the proposed diagnostics (solid line) and the results of solving the inverse problem (15)-(18) (dotted line)

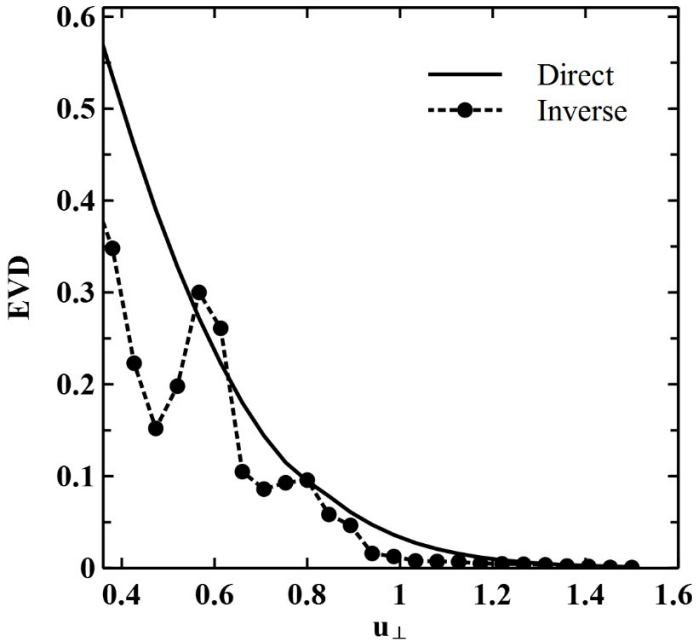

Figure 8: The EVD as a function of perpendicular to the magnetic field component of the momentum $u = p/mc$ for the fixed values $u_\parallel = 0.1$ and $\rho = 0$: direct data (4), (6), (7) (solid line) and the result of solving the inverse problem (15)-(18) (dotted line)

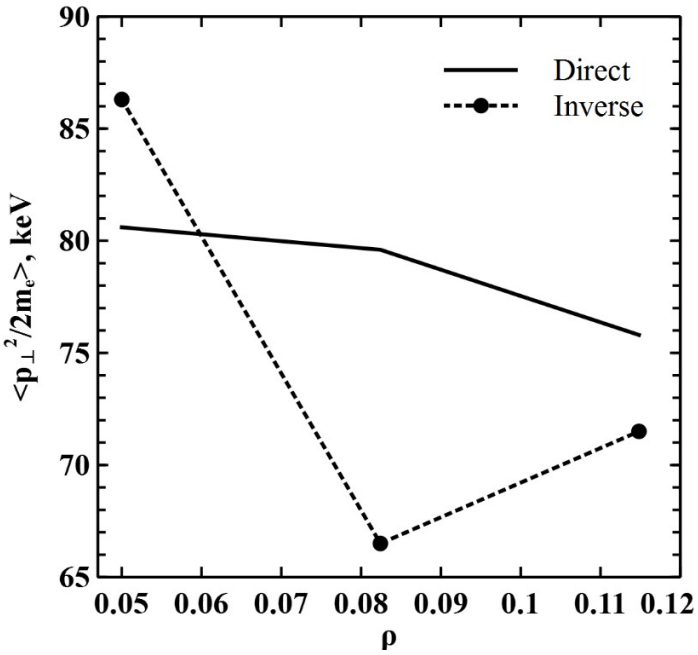

Figure 9: Averaged value of perpendicular kinetic energy as a function of the magnetic surface label ρ: direct calculation for EVD (4), (6), (7) (solid line) and the results of solving the inverse problem (15)-(18) (dashed line)

We have to note that the weak dependence of the emissivity of EC radiation of a single electron (Fig. 6) on the parallel to the magnetic field component of the electron momentum did not allow us to correctly restore the parameters of the parallel kinetic energy.

4. CONCLUSIONS

An analysis of the high-number-harmonic EC radiation from a hot fusion-reactor plasmas, expected under condition of a strong auxiliary heating (e.g. in tokamak DEMO, a next step after tokamak ITER), enabled us to suggest a new method of spectroscopic diagnostics of the average transverse-to-magnetic-field momentum of the non-thermal component of the electron velocity distribution (EVD). The method is based on solving an inverse problem for reconstruction of the EVD in parallel and perpendicular to magnetic field components of electron momentum at high and moderate energies responsible for the emission of the high-number-harmonic EC radiation. The well-known difficulty of solving such a problem in the case of arbitrary EVD (complexity of spectrum, radiative transfer effects for low-number harmonics and nonlocality of transport for high-number harmonics, etc.) restricted the capability to reconstruct the main parameters of the EVD to those parameters which are most sensitive to EC radiation, namely, to average transverse-to-magnetic-field momentum of non-thermal electrons. However, the combination of such a diagnostic with those which can determine the parameters of the bulk Maxwellian plasma (like Thomson diagnostics) may provide a powerful tool for spectroscopic plasma diagnostics of fusion-reactor plasmas.

Acknowledgements

The authors are grateful to E. E. Mukhin (Ioffe Physical Technical Institute) for stimulating the interest to spectroscopic diagnostics of electron velocity distribution in DEMO, V. I. Poznyak, (NRC "Kurchatov Institute"), for helpful discussion of EC diagnostics experimental issues. The present work is supported by the State Corporation ROSATOM and the Council of the Russian Federation Presidential Grants for State Support of Leading Scientific Schools (grant No. NSh_65382.2010.2).

References

[1] G. Bekefi, Radiation Processes in Plasmas, New York: Wiley, (1966).

[2] M. Bornatici, R. Cano, O. De Barbieri, and F. Engelmann, "Electron Cyclotron Emission and Absorption in Fusion Plasmas", *Nuclear Fusion*, **23**, (1983), 1153.

[3] P. V. Minashin, A. B. Kukushkin, and V. I. Poznyak, "Reconstruction of Superthermal Electron Velocity Distribution Function from Electron Cyclotron Spectra at Down-Shifted Frequencies in Tokamak T-10", *EPJ Web of Conferences*, **32**, (2012), 01015.

[4] P. V. Minashin, A. B. Kukushkin, and V. I. Poznyak, "A Model for Electron Cyclotron Spectra at Down-Shifted Frequencies and Reconstruction of Superthermal Electron Velocity in Tokamak T-10", Proc. *39th EPS Conference on Plasma Physics*, Stockholm, Sweden, **36F**, (2012), P1.039, ECA.

[5] I. H. Hutchinson, and K. Kato, "Diagnosis of Mildly Relativistic Electron Distributions by Cyclotron Emission ", *Nuclear Fusion*, **26**, (1986), 179-191.

[6] S. Tamor, "Calculation of Energy Transport by Cyclotron Radiation in Fusion Plasmas", *Nuclear Technology/Fusion*, **3**, (1983), 293.

[7] A. B. Kukushkin, "Heat Transport by Cyclotron Waves in Plasmas with Strong Magnetic Field and Highly Reflecting Walls", Proc. *14th IAEA Conference on Plasma Physics and Controlled Nuclear Fusion Research*, Wuerzburg, Germany, **2**, (1992), 35-45, IAEA.

[8] F. Albajar, M. Bornatici, and F. Engelmann, "Electron Cyclotron Radiative Transfer in Fusion Plasmas", *Nuclear Fusion*, **42**, (2002), 670-678.

[9] F. Albajar, M. Bornatici, and F. Engelmann, "RAYTEC: A New Code for Electron Cyclotron Radiative Transport Modelling of Fusion Plasmas", *Nuclear Fusion*, **49**, (2009), 115017.

[10] F. Albajar, M. Bornatici, G. Cortes, and J. Dies, *et al*., "Importance of Electron Cyclotron Wave Energy Transport in ITER", *Nuclear Fusion*, **45**, (2005), 642-648.

[11] A. B. Kukushkin, P. V. Minashin, and A. R. Polevoi, "Impact of Magnetic Field Inhomogeneity on Electron Cyclotron Radiative Loss in Tokamak Reactors", *Plasma Physics Reports*, **38**, (2012), 211-220.

[12] A. B. Kukushkin, P. V. Minashin, and A. R. Polevoi, "Limit of Electron Cyclotron Radiation in ITER Long Pulse Operation", Proc. *38th EPS Conference on Plasma Physics*, Strasbourg, France, **35G**, (2011), P4.072, ECA.

[13] A. R. Polevoi, S. Y. Medvedev, T. Casper, and Y. V. Gribov, *et al*., "Assessment of Operational Space for Long-Pulse Scenarios in ITER", Proc. *37th EPS Conference on Plasma Physics*, Dublin, Ireland, **34A**, (2010), P2.187, ECA.

[14] K. V. Cherepanov, and A. B. Kukushkin, "Influence of Suprathermal Electrons Kinetics on Cyclotron Radiation Transport in Hot Toroidal Plasmas", Proc. *20th IAEA Fusion Energy Conference*, Vilamoura, Portugal, TH/P6-56, (2004).

[15] A. B. Kukushkin, K. V. Cherepanov, L. K. Kuznetsova, and E. Westerhof, "Influence of ECCD/ECRH-Produced Superthermal Electrons on Transport of Plasma's Electron Cyclotron Radiation in Tokamak-Reactor", Proc. *14th Joint Workshop on Electron Cyclotron Emission and Electron Cyclotron Heating*, Santorini, Greece, 374, (2006), Heliotopos Conferences Ltd.

[16] F. Albajar, M. Bornatici, and F. Engelmann, "EC Radiative Transport in Fusion Plasmas with an Anisotropic Distribution of Suprathermal Electrons", Proc. *16th Joint Workshop "Electron Cyclotron Emission And Electron Cyclotron Resonance Heating"*, Sanya, China, (2010), 215-221.

[17] K. V. Cherepanov, and A. B. Kukushkin, "Self-Consistent Simulation of Electron Cyclotron Radiation Transport and Superthermal Electron Kinetics in Hot Tokamak Plasmas", Proc. *32thEPS Conference on Plasma Physics*, Tarragona, Spain, **29C**, (2005), P-2.117, ECA.

[18] P. V. Minashin, and A. B. Kukushkin, "Algorithm of Self-Consistent Calculation of EC Losses and Kinetics of ECRH/ECCD in Tokamak-Reactors", Proc. *40th EPS Conference on Plasma Physics*, Espoo, Finland, P4.176, (2013).

[19] R. W. Harvey, and M. G. McCoy, "The CQL3D Code", Proc. *IAEA Technical Committee Meeting on Advances in Simulation and Modeling of Thermonuclear Plasmas*, Montreal, Canada, (1992), 489-526, IAEA Institute of Physics Publishing.

[20] G. Zhuang, R. Behn, I. Klimanov, and P. Nikkola, *et al*., "Influence of Non-Maxwellian Velocity Distributions During ECRH and ECCD on Electron Temperature Measurements by Thomson Scattering", *Plasma Physics and Controlled Fusion*, **47**, (2005), 1539.

[21] J. Garcia, G. Giruzzi, J. F. Artaud, and V. Basiuk, *et al*., "Analysis of DEMO Scenarios with the CRONOS Suite of Codes", *Nuclear Fusion*, **48**, (2008), 075007.

[22] V. Basiuk, J. F. Artaud, F. Imbeaux, and X. Litaudon, *et al*., "Simulations of Steady-State Scenarios for Tore Supra Using the CRONOS Code", *Nuclear Fusion*, **43**, (2003), 822.

[23] A. B. Kukushkin, and P. V. Minashin, "Influence of Magnetic Field Inhomogeneity on Electron Cyclotron Power Losses in Magnetic Fusion Reactor", Proc. *36thEPS Conference on Plasma Physics*, Sofia, Bulgaria, **33E**, (2009), P-4.136, ECA.

[24] A. B. Kukushkin, P. V. Minashin, and A. R. Polevoi, "Electron Cyclotron Power Losses in ITER for 2D Profile of Magnetic Field", Proc. *23rd IAEA Fusion Energy Conference*, Daejon, South Korea, (2010), ITR/P1-34.

[25] F. Albajar, M. Bornatici, F. Engelmann, and A. B. Kukushkin, "Benchmarking of Codes for Calculating Local Net EC Power Losses in Fusion Plasmas", *Fusion Science and Technology*, **55**, (2009), 76-83.

[26] A. B. Kukushkin, and P. V. Minashin, "Benchmarking of Codes for Spatial Profiles of Electron Cyclotron Losses with Account of Plasma Equilibrium in Tokamak Reactors", Proc. *24th IAEA Fusion Energy Conference*, San Diego, USA, TH/P6-25, (2012).

[27] G. V. Pereverzev, and P. N. Yushmanov, "ASTRA – Automated System for Transport Analysis in a Tokamak", Report IPP 5/98, (2002), Garching.

[28] S. Tamor, "A Simple Fast Routine for Computation of Energy Transport by Synchroton Radiation in Tokamaks and Similar Geometries", Report SAI-023-81-189LJ/LAPS-72, La Jolla, CA, (1981).

[29] B. A. Trubnikov, Plasma Physics and the Problem of Controlled Thermonuclear Reactions Series, (Ed.), M.A. Leontovich, New York: Pergamon Press, **3**, (1959), 122.